

# Generation of Human Adult Mesenchymal Stromal/Stem Cells Expressing Defined Xenogenic Vascular Endothelial Growth Factor Levels by Optimized Transduction and Flow Cytometry Purification

Uta Helmrich, Ph.D.,<sup>1</sup> Anna Marsano, Ph.D.,<sup>2</sup> Ludovic Melly, M.D.,<sup>1</sup> Thomas Wolff, M.D.,<sup>1</sup> Liliane Christ, B.S.,<sup>1</sup> Michael Heberer, M.D.,<sup>1,2</sup> Arnaud Scherberich, Ph.D.,<sup>2</sup> Ivan Martin, Ph.D.,<sup>2</sup> and Andrea Banfi, M.D.<sup>1</sup>

Adult mesenchymal stromal/stem cells (MSCs) are a valuable source of multipotent progenitors for tissue engineering and regenerative medicine, but may require to be genetically modified to widen their efficacy in therapeutic applications. For example, overexpression of the angiogenic factor vascular endothelial growth factor (VEGF) at controlled levels is an attractive strategy to overcome the crucial bottleneck of graft vascularization and to avoid aberrant vascular growth. Since the regenerative potential of MSCs is rapidly lost during *in vitro* expansion, we sought to develop an optimized technique to achieve high-efficiency retroviral vector transduction of MSCs derived from both adipose tissue (adipose stromal cells, ASCs) or bone marrow (BMSCs) and rapidly select cells expressing desired levels of VEGF with minimal *in vitro* expansion. The proliferative peak of freshly isolated human ASCs and BMSCs was reached 4 and 6 days after plating, respectively. By performing retroviral vector transduction at this time point, >90% efficiency was routinely achieved before the first passage. MSCs were transduced with vectors expressing rat VEGF<sub>164</sub> quantitatively linked to a syngenic cell surface marker (truncated rat CD8). Retroviral transduction and VEGF expression did not affect MSC phenotype nor impair their *in vitro* proliferation and differentiation potential. Transgene expression was also maintained during *in vitro* differentiation. Furthermore, three subpopulations of transduced BMSCs homogeneously producing specific low, medium, and high VEGF doses could be prospectively isolated by flow cytometry based on the intensity of their CD8 expression already at the first passage. In conclusion, this optimized platform allowed the generation of populations of genetically modified MSCs, expressing specific levels of a therapeutic transgene, already at the first passage, thereby minimizing *in vitro* expansion and loss of regenerative potential.

## Introduction

ADULT MESENCHYMAL stem/stromal cells (MSCs) are a population of multipotent progenitors, capable of generating bone, cartilage, fat, and possibly other mesodermal tissues and represent a fundamental tool in regenerative medicine.<sup>1,2</sup> MSCs have been described in many tissues as a pericyte-like population in close association with blood vessels,<sup>3</sup> raising the intriguing possibility that they may reside in the vascularized stroma of every tissue. However, the most commonly used and characterized MSCs are derived from bone marrow (BMSCs) and adipose tissue (adipose stromal cells, ASCs), due to their abundance and ease of harvesting.<sup>4,5</sup>

Despite their potential, it may be desirable to genetically modify MSCs in order to increase their survival and/or differentiation in therapeutic applications. For example, sponta-

neous vascularization of tissue-engineered grafts *in vivo* is too slow to allow survival of progenitors in constructs larger than a few millimeters. To overcome this bottleneck in the generation of clinical-size grafts, it is necessary to increase their ability to rapidly attract a vascular supply from the host, for example, by overexpressing an angiogenic factor from the implanted progenitors.<sup>6-8</sup>

Vascular endothelial growth factor (VEGF) is the master regulator of vascular growth both in embryonic development and adult tissues.<sup>9</sup> When expressed at the appropriate dose, VEGF can start the complex cascade of events leading to the formation of stable and functional new blood vessels.<sup>10</sup> However, sustained expression is required for about 4 weeks in order to avoid regression of newly induced unstable vessels.<sup>11,12</sup>

Nonintegrating gene therapy vectors are progressively lost during cell expansion and lead to short-term and

<sup>1</sup>Cell and Gene Therapy, and <sup>2</sup>Tissue Engineering, Departments of Biomedicine and Surgery, Basel University Hospital, Basel, Switzerland.

variable expression. Gene expression is thus less controllable, making it challenging to achieve a desired therapeutic effect. Integrating vectors, such as retroviral vectors on the other hand, replicate with the host genome and ensure constant expression throughout cell expansion.<sup>13,14</sup>

MSCs have been shown to rapidly lose their differentiation potential during *in vitro* expansion.<sup>15,16</sup> Therefore it is crucial that genetic modification takes place both with high efficiency, in order to minimize the need for cell selection, and with minimal *in vitro* manipulation of progenitors.

Therefore, here we sought to develop an optimized technique to achieve rapid and high-efficiency transduction of primary MSCs from both bone marrow and adipose tissue with minimal *in vitro* expansion, together with high-throughput purification of the progenitor populations expressing specific transgene levels based on fluorescence-activated cell sorting (FACS). The study of *in vivo* vascularization of critical-size osteogenic grafts seeded with human MSCs requires a nude rat model, due both to the dimensions of the constructs and the need to avoid rejection of human cells. However, nude rats are tolerant to xenogenic cells, but not secreted molecules, and can develop antibodies against them. Therefore, we generated genetically modified human MSCs overexpressing rat VEGF in view of subsequent *in vivo* experiments in rats with this tool. Greater than 90% transduction efficiency of freshly isolated BMSCs and ASCs could be routinely achieved and FACS purification was possible already at the time of the first passage, while no loss of *in vitro* proliferation and differentiation potential was caused by either the genetic modification or the FACS sorting.

## Materials and Methods

### MSC isolation and culture

Human primary ASCs and BMSCs were isolated from liposuction and bone marrow aspirates, respectively. The aspirates were obtained from healthy donors as previously described after informed consent by the patients and approval by the local ethical committee. Briefly, subcutaneous adipose tissue was digested in 0.075% type-II collagenase (Worthington) in phosphate-buffered saline (PBS) and plated at a density of  $5.5 \times 10^3$  nucleated cells/cm<sup>2</sup>.<sup>17</sup> Bone marrow was subjected to red blood cell lysis<sup>18</sup> and plated at a density of  $10^5$  nucleated cells/cm<sup>2</sup>. Both ASCs and BMSCs were cultured in  $\alpha$ -MEM supplemented with 10% fetal bovine serum (FBS) (Gibco) and 5 ng/mL fibroblast growth factor (FGF)-2 (BD Biosciences). Cells were passaged when 80% confluent and replated at a density of  $3 \times 10^3$  cells/cm<sup>2</sup>.

Colony forming efficiency assays were performed on freshly isolated cells as described.<sup>19</sup> The proliferation rate was determined by counting the number of cells at every passage with a Neubauer chamber (Roth), determining the number of population doublings from the previous passage<sup>19</sup> and plotting the cumulative doublings against the time in culture.

### Myoblast culture

Primary C57Bl/6 mouse myoblasts were cultured on collagen-coated dishes in medium consisting of 40% F10, 40% low-glucose Dulbecco's modified Eagle's medium (both

Sigma), supplemented with 20% FBS and 2.5 ng/mL FGF-2, as previously described.<sup>20</sup>

### Cell cycle analysis

The proportion of actively cycling cells was determined by measuring their nuclear DNA content by flow cytometry after staining with propidium iodide as described.<sup>21</sup> The data were analyzed using the cell cycle analysis tool from FlowJo Software (Tree Star) using the Watson model.<sup>22</sup> ASCs ( $n=4$  donors) and BMSCs ( $n=3$  donors) from duplicate dishes were analyzed at each time point.

### Retroviral transduction

The optimization experiments were performed with frozen aliquots of a pooled stock of retroviral vector supernatant, to ensure the same titer in all conditions. Subsequent experiments were performed with fresh viral vector supernatants. Primary MSCs were transduced with previously described retroviral vectors, carrying the gene for rat VEGF<sub>164</sub> linked through an internal ribosomal entry site (IRES) to a truncated version of the FACS-quantifiable cell surface marker truncated rat CD8a,<sup>23</sup> according to a high-efficiency protocol.<sup>24</sup> Briefly, MSCs were cultured in 60-mm dishes and were incubated with retroviral vector supernatants supplemented with 8  $\mu$ g/mL polybrene (Sigma-Aldrich) for 5 min at 37°C and centrifuged at 1100g for 30 min at room temperature in the dishes, followed by fresh medium replacement. After initial optimization, all subsequent experiments were carried out with cells transduced twice per day for a total of 4 infection rounds.

### Flow cytometry

CD8a expression was assessed by staining with a fluorescein isothiocyanate-conjugated anti-rat CD8a antibody (clone OX-8; BD Pharmingen), using previously optimized staining conditions to ensure complete saturation of the CD8a molecules expressed on all cells in the heterogeneous transduced population,<sup>23</sup> that is, 2  $\mu$ g of antibody/10<sup>6</sup> cells in 200  $\mu$ L of PBS with 5% bovine serum albumin.

Expression of MSC surface markers was assessed by staining with specific antibodies against CD31 (clone WM59; BD Pharmingen), CD34 (clone 581; BD Pharmingen), KDR/VEGFR2 (clone 89106; R&D Systems), CD73 (clone AD2; BD Pharmingen), CD90 (clone 5E10; BD Pharmingen), and CD105 (clone SN6; AbD Serotec). All antibodies were used at a 1:20 dilution except for CD90 (1:100). Aspecific binding was measured by staining with appropriate isotype control antibodies. Data were acquired with a FACSCalibur flow cytometer (Becton Dickinson) and analyzed using FlowJo software (Tree Star). Cell sorting was performed with the Influx cell sorter (Becton Dickinson).

### MSC immunostaining

Fifty percent confluent MSC cultures were fixed with 4% formalin, blocked for 1 h with 10% calf serum in PBS, and incubated with an antibody against rat CD8a (clone OX-8, BD Pharmingen; 1:200), followed by an Alexa 488-conjugated chicken anti-mouse IgG (Invitrogen; 1:500). Nuclei were stained with 4',6-diamidino-2-phenylindole (DAPI) (Invitrogen).

### *In vitro differentiation*

Adipogenic differentiation was induced as previously described.<sup>17</sup> Briefly, subconfluent cell layers were treated with 10 µg/mL insulin, 10<sup>-5</sup> M dexamethasone, 100 µM indomethacin, and 500 µM 3-isobutyl-1-methyl xanthine for 72 h and subsequently with 10 µg/mL insulin for 24 h, repeating this 96-h treatment cycle four times. Lipid droplets were detected with Oil Red-O staining.

Osteogenic differentiation was induced by culturing MSCs with  $\alpha$ -MEM supplemented with 10% FBS, 100 nM dexamethasone, 10 mM  $\beta$ -glycerophosphate, and 0.05 mM ascorbic acid-2-phosphate for 3 weeks, as previously described.<sup>17</sup> Calcium deposits were detected with Alizarin Red staining.

### *Quantitative real-time reverse transcriptase polymerase chain reaction*

Total mRNA was isolated using the RNeasy Mini Kit (Qiagen) and cDNA was synthesized with the Superscript III Reverse Transcriptase (Invitrogen).

Quantitative real-time reverse transcriptase polymerase chain reaction (qRT-PCR) was performed on a 7300 AB thermocycler (Applied Biosystem) to quantify the expression of the following genes: human *cbfa-1/Runx2* (Forward: CGTTACCCGCCATGACAGTA; Reverse: GCCTCAA GGTGGTAGCCC; Probe: CCACAGTCCCATCTGGTACC TCTCCG; primers=300 nM and probe=100 nM)<sup>25</sup>; *PPAR- $\gamma$*  (Applied Biosystems assay Hs00234592\_mL; primers=900 nM and probe=250 nM). To quantify expression of the retroviral cassette, a specific primers-and-probe set was designed with the Primer Express 3 software (Applied Biosystems) to recognize the IRES sequence (Forward: GCTCTCCTCAAGCGTATTCAACA; Reverse: CCCAGAT CAGATCCCATAACA; Probe: CTGAAGGATGCCCAGAAG GTACCCCA; primers=400 nM and probe=400 nM). Glyceraldehyde 3-phosphate dehydrogenase was used as a housekeeping gene (Forward: TAAAAGCAGCCCTGGTG ACC; Reverse: ATGGGGAAGGTGAAGGTCG; Probe: CGCCAATACGACCAAATCCGTTGAC; primers=300 nM and probe=150 nM).<sup>26</sup> Two independent cDNA samples/condition/donor were analyzed in triplicate with the following cycling parameters: 50°C for 2 min, followed by 95°C for 10 min and 45 cycles of denaturation at 95°C for 15 s and annealing/extension at 60°C for 1 min.

### *Enzyme-linked immunosorbent assay*

VEGF production was quantified in cell culture supernatants using a Quantikine rat VEGF immunoassay enzyme-linked immunosorbent assay (ELISA) kit (R&D Systems). One milliliter of fresh medium was incubated on MSCs cultured in 60-mm dishes (for expansion cultures) or in six-wells (at the end of differentiation experiments) in duplicate for 4 h, filtered, and frozen. Results were normalized by the number of cells in each dish and the time of incubation.

### *Statistics*

Data are presented as means  $\pm$  standard error. The significance of differences in multiple comparisons was evaluated using one-way analysis of variance followed by the Bonferroni test.  $p < 0.05$  was considered statistically significant.

## **Results**

### *Optimization of MSC transduction*

Since retroviral vectors efficiently transduce only dividing cells, we first sought to determine the earliest time after isolation and plating when ASCs and BMSCs enter the cell cycle and proliferation is at its peak. Cell cycle analysis was performed on samples from 3 independent donors every day from the initial plating to the time of first confluence, which was reached consistently by day 12 and 14 for ASCs and BMSCs, respectively. ASCs reproducibly reached a proliferation peak 4 days after isolation (52.2%  $\pm$  5.0% of cycling cells) that was maintained until day 7, after which replication declined with increasing confluence (Fig. 1A). BMSCs displayed a higher variability in the first days, but their growth trend was similar, proliferation reached its maximum on day 6 (54.7%  $\pm$  5.5%) and declined after day 10 (Fig. 1B).

Based on these results, we determined the optimal time to start transduction to be on day 4 after isolation for ASCs and day 6 for BMSCs. Cells were transduced twice per day up to six times with a retroviral vector expressing the cell surface marker CD8 and the transduction efficiency was evaluated after each round by FACS quantification of the CD8-positive cells. The majority of the increase in the number of transduced cells took place during the first four rounds for both ASCs and BMSCs (Fig. 1C, D), while the last two rounds only contributed marginal improvement. Therefore, it was determined that four rounds of transduction would provide a suitable balance between efficacy and cell manipulation and this protocol was used to generate all cell populations for further analysis described below.

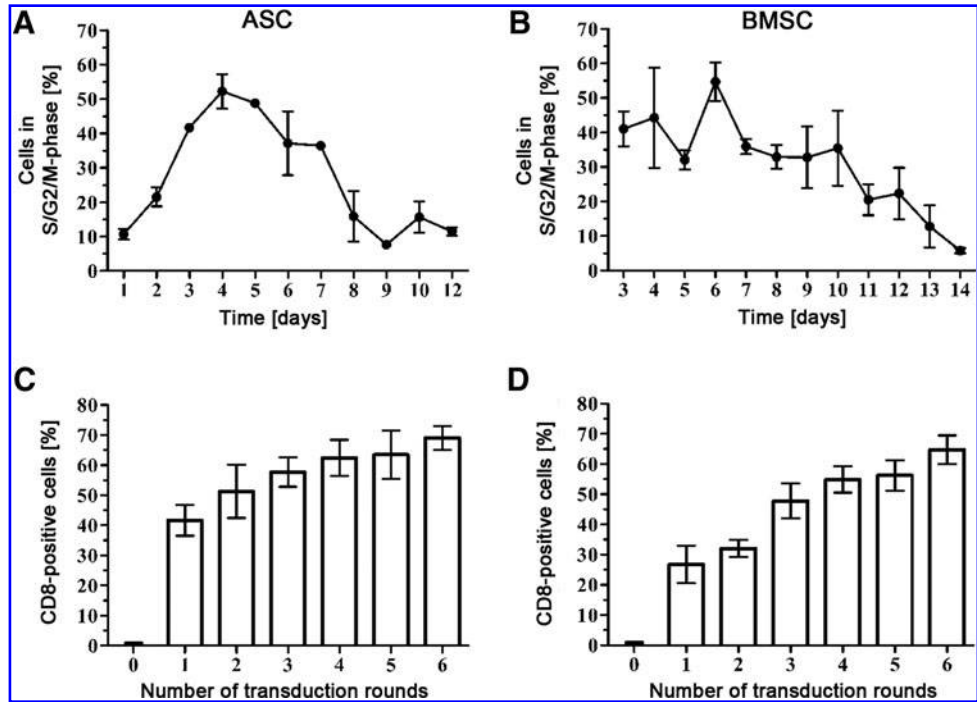
### *Generation of FACS-sortable MSCs*

Freshly isolated ASCs and BMSCs were transduced according to the optimized protocol with a bicistronic retroviral vector coexpressing rat VEGF<sub>164</sub> (VEGF) and a truncated version of rat CD8a (CD8) as a FACS-quantifiable cell surface marker, joined through an internal ribosomal entry site (IRES) that allows the translation of two proteins from the same mRNA at a fixed ratio<sup>27</sup> (Fig. 2). A retroviral vector expressing only CD8 was used to generate control cells. These genetically modified populations were used for further analysis (Fig. 2).

Using freshly produced viral vector supernatants with the optimized protocol described previously, a transduction efficiency >90% was routinely achieved (Fig. 3A, B). Upon reaching the first confluence, MSCs were FACS purified in order to remove nontransduced cells and to yield pure CD8-positive populations (Fig. 3A, B), which were replated for all subsequent experiments. Neither sorting nor transduction affected the morphology of ASCs and BMSCs, which exhibited a spindle-shaped phenotype similar to that of the corresponding naive cells (Fig. 3C, D, bright field). Detection of membrane CD8 by immunofluorescent staining confirmed the high efficiency of transduction (Fig. 3C, D, unsorted) and the lack of nontransduced cells after sorting (Fig. 3C, D, sorted).

We further investigated whether transduction or VEGF expression could change the phenotype of MSC populations or cause the expansion of endothelial subpopulations. For this purpose the expression of surface markers specific for

**FIG. 1.** Optimization of MSC retroviral vector transduction. The proportion of ASCs (A) and BMSCs (B) in active proliferation (S/G2/M phases) was assessed by flow cytometry analysis of nuclear DNA content after staining with propidium iodide during the first 12 to 14 days after initial plating ( $n=3$  each). The transduction efficiency of ASCs (C) and BMSCs (D) was assessed as a function of infection rounds ( $n=3$  each). The amount of CD8-positive cells was determined by FACS after up to six rounds of transduction with a CD8-expressing retroviral vector. Naive MSCs were used as negative control (0 rounds). MSCs, mesenchymal stromal/stem cells; ASCs, adipose stromal cells; FACS, fluorescence-activated cell sorting; BMSCs, bone marrow-derived MSCs.



mesenchymal (CD105, CD90, and CD73) and endothelial (CD31, CD34, and VEGFR2) cells was analyzed by flow cytometry. Naive ASCs and BMSCs were compared with mock-transduced cells (centrifuged only) and with CD8- or VEGF-expressing transduced and sorted cells. As shown in Table 1, first-passage naive ASCs and BMSCs were almost uniformly positive for all the analyzed mesenchymal markers and contained less than 0.5% of endothelial cells. No significant changes in the mesenchymal phenotype of manipulated MSCs were caused by transduction and sorting or by VEGF expression, nor was the ratio of endothelial cells increased in any condition.

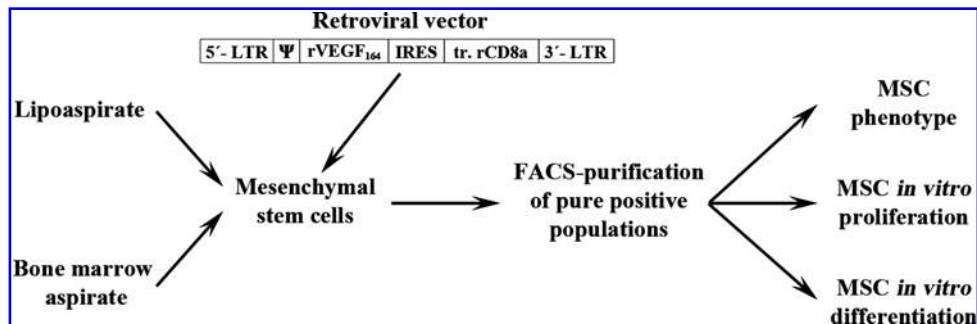
*In vitro proliferation and differentiation of genetically modified MSCs*

The effects of transduction and FACS purification on MSC proliferative potential were assessed by measuring the cumulative population doublings of CD8- and VEGF-expressing

ASCs and BMSCs for eight and nine passages after sorting, respectively. These were compared with naive cells and mock-transduced cells that were subjected to the physical manipulation involved in the transduction protocol, that is, centrifugation for 30' in the dish, but in the absence of viral vector particles. Both transduced ASC and BMSC populations proliferated more slowly than the naive and centrifuged MSCs during the first two passages after sorting (Fig. 4). However, this effect was temporary and growth of transduced MSCs resumed at the same rate as control cells approximately 10 days after the sorting (Fig. 4). Therefore, transduction and sorting did not affect the intrinsic proliferative potential of MSCs.

The differentiation potential of the same ASC and BMSC populations toward the adipogenic and osteogenic lineages was determined *in vitro* after the first passage and FACS purification. Mock-transduced, CD8- and VEGF-expressing ASCs (Fig. 5A) and BMSCs (Fig. 5C) were able to differentiate into both lineages similarly to the naive MSCs.

**FIG. 2.** Study design. ASCs and BMSCs were isolated and transduced with a bicistronic retroviral vector coexpressing rat VEGF<sub>164</sub> (rVEGF<sub>164</sub>) and a truncated version of rat CD8a (tr. rCD8a). LTR=retroviral long terminal repeats; Ψ= packaging signal; IRES= internal ribosomal entry site. CD8-positive MSCs were FACS sorted to generate pure populations of transduced cells and were analyzed to determine the effects of retroviral transduction and transgene expression on their phenotype, as well as their *in vitro* proliferation and differentiation potential. VEGF, vascular endothelial growth factor.



and transgene expression on their phenotype, as well as their *in vitro* proliferation and differentiation potential. VEGF, vascular endothelial growth factor.

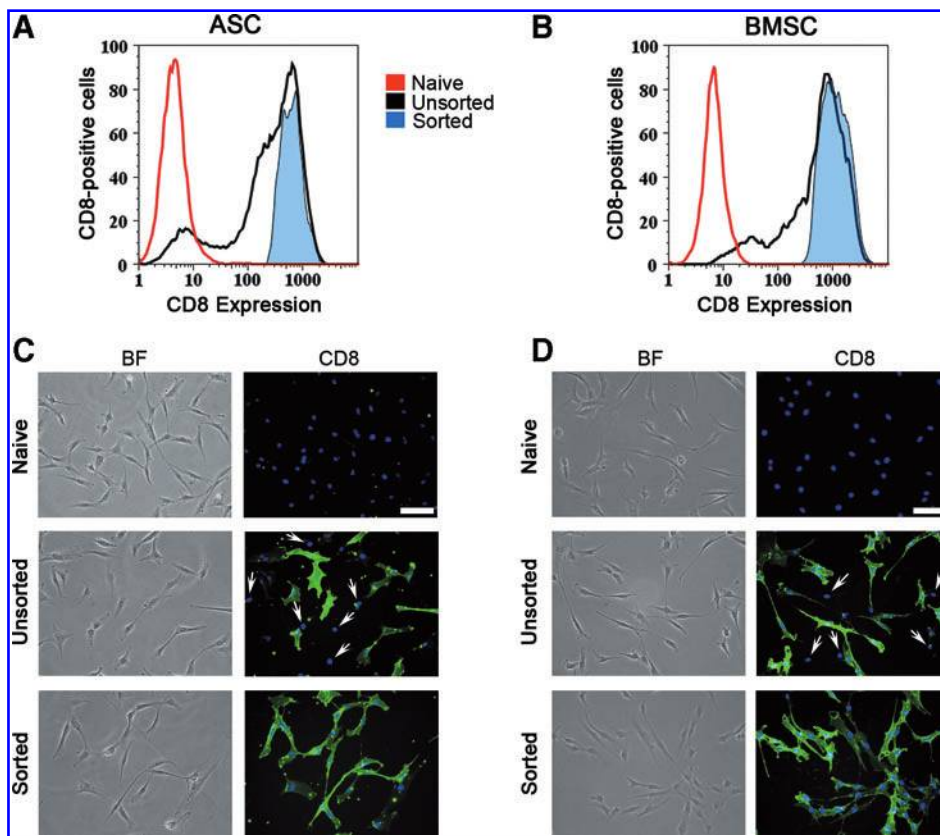


**FIG. 3.** FACS purification of transduced MSCs. Representative FACS plots show that both ASCs (A) and BMSCs (B) were transduced with >90% efficiency (black plots) and that pure CD8-positive populations were obtained after sorting (tinted blue plots). Control naive cells = red plots. Microscopic images of naive or VEGF-expressing ASCs (C) and BMSCs (D), either before (unsorted) or after (sorted) FACS purification. BF = bright field images; CD8 = cells immunostained with an anti-CD8 antibody (green) and DAPI (nuclei, in blue). White arrows indicate the nuclei of CD8-negative cells in the unsorted populations (n = 3 each). Size bar = 100 μm. DAPI, 4',6-diamidino-2-phenylindole. Color images available online at [www.liebertonline.com/tec](http://www.liebertonline.com/tec)

Interestingly, in ASCs from one donor with poor intrinsic osteogenic differentiation potential (Fig. 5B), VEGF expression actually increased osteogenic differentiation compared with naive, mock-transduced and CD8-expressing cells (Fig. 5B). Differentiation was confirmed by quantifying the expression of transcription factors that are responsible for initiating adipogenesis (PPAR-γ, Fig. 5D, E) and osteogenesis (Runx2, Fig. 5F, G) by qRT-PCR. The results confirmed that ASC and BMSC differentiation along both lineages was not

impaired by retroviral transduction, FACS purification, or VEGF expression.

*Transgene expression is maintained after cell differentiation*

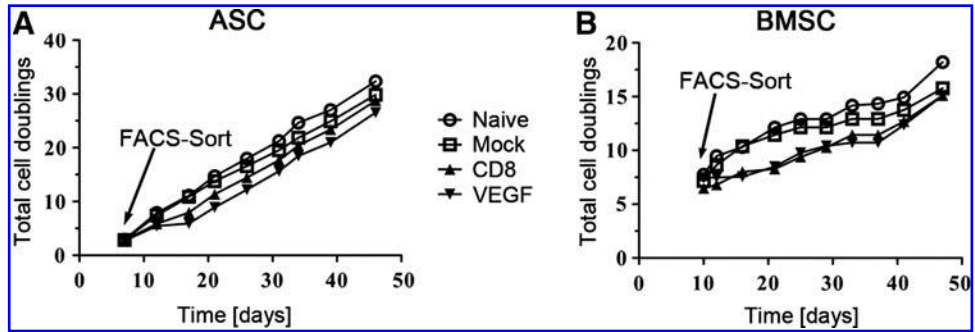
Retroviral vectors integrate in the host genome and their level of expression can be affected by remodeling of the surrounding chromatin that accompanies gene activation

**TABLE 1.** EXPRESSION OF ENDOTHELIAL AND MESENCHYMAL MARKERS BY NAIVE AND TRANSDUCED ADULT MESENCHYMAL STROMAL/STEM CELLS

		% of positive cells in ASC populations			
		Naive	Mock	CD8	VEGF
Endothelial markers	CD31+ /CD34+	0.2±0.1	0.2±0.1	0.3±0.2	0.1±0.1
	VEGFR2+	0.0±0.0	0.1±0.1	0.5±0.2	0.0±0.0
Mesenchymal markers	CD73+	94.4±5.0	95.7±3.5	91.2±8.4	91.6±8.1
	CD90+	94.4±5.2	94.9±4.7	90.6±8.9	89.3±10.1
	CD105+	93.6±4.7	91.9±3.9	87.7±6.5	86.2±6.9
		% of positive cells in BMSC populations			
		Naive	Mock	CD8	VEGF
Endothelial Markers	CD31+ /CD34+	0.0±0.0	0.0±0.0	0.0±0.0	0.0±0.0
	VEGFR2+	0.0±0.0	0.5±0.4	0.0±0.0	0.1±0.1
Mesenchymal markers	CD73+	99.6±0.1	99.8±0.1	99.7±0.1	99.7±0.1
	CD90+	89.2±3.5	89.0±3.2	91.8±3.1	93.1±1.5
	CD105+	98.9±0.4	98.3±1.4	99.2±0.3	99.0±0.5

BMSCs, bone marrow-derived mesenchymal stromal/stem cells; ASCs, adipose stromal cells.

**FIG. 4.** *In vitro* proliferation of transduced MSCs. The *in vitro* proliferative potential of CD8- and VEGF-expressing ASCs (A) and BMSCs (B) was not impaired compared with that of naive and mock-transduced cells over nine passages after FACS sorting ( $n=3$  each).



and repression during differentiation.<sup>28</sup> Therefore, we assessed the stability of transgene expression by transduced and FACS-purified MSCs during differentiation.

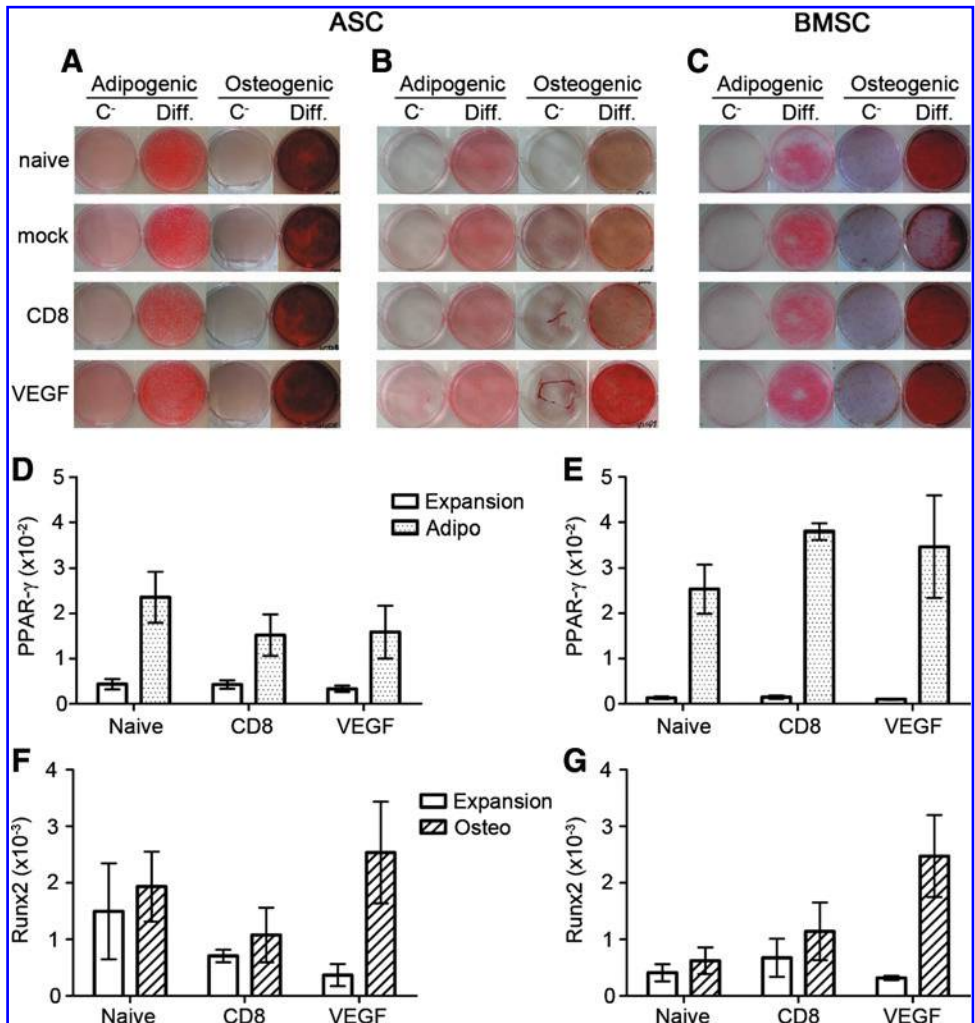
Transgene mRNA levels were quantified by qRT-PCR of the IRES sequence, which is common to the expression cassettes in both retroviral vectors used (CD8 and VEGF), so that the use of a single pair of primers allowed comparisons between all cell populations (Fig. 6A, B). VEGF protein was measured by ELISA (Fig. 6C, D). Both assays indicated that transgene expression did not decline during *in vitro* adipo-

genic or osteogenic differentiation compared with cells in expansion medium, and that in some instances it actually increased.

*FACS purification of MSCs expressing specific VEGF levels*

To rapidly purify homogeneous populations expressing desired levels of VEGF, we employed a technology that we recently developed with transduced skeletal myoblasts.<sup>23,29</sup>

**FIG. 5.** *In vitro* differentiation of transduced MSCs. Naive, mock-transduced, CD8- and VEGF-expressing MSCs were differentiated *in vitro* toward the adipogenic and osteogenic lineages. (A–C) Oil Red-O staining (adipogenic) and Alizarin Red staining (osteogenic) of control (C-) or differentiated (Diff.) ASCs (A, B, from two different donors) and BMSCs (C) ( $n=4$  each). Differentiation was confirmed by quantifying the expression of PPAR- $\gamma$  (adipogenesis, D, E) and Runx2 (osteogenesis, F, G) in expansion and differentiation conditions by quantitative real-time PCR ( $n=3$  each). The graphs show relative expression compared with that of the housekeeping gene GAPDH. PCR, polymerase chain reaction; GAPDH, glyceraldehyde 3-phosphate dehydrogenase. Color images available online at [www.liebertonline.com/tec](http://www.liebertonline.com/tec)



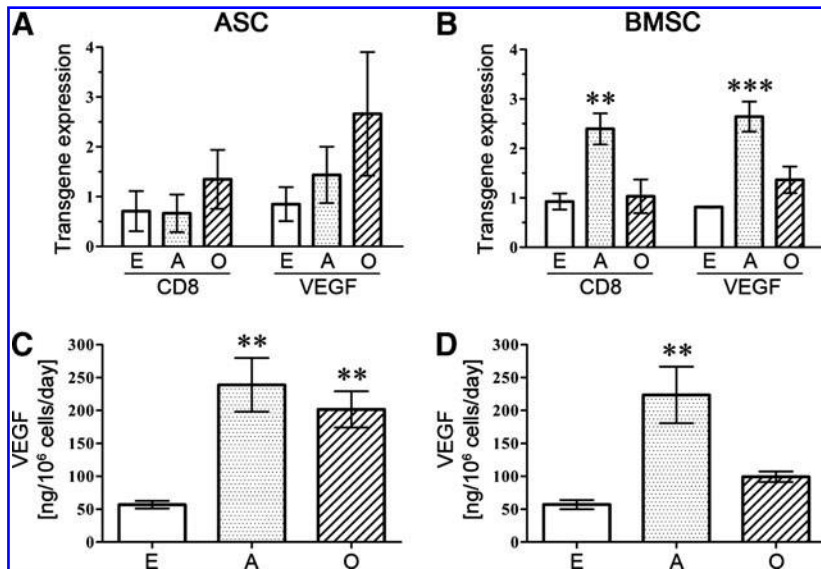


**FIG. 6.** Transgene expression after *in vitro* differentiation. Transgene expression was quantified in expansion culture (E) or after adipogenic (A) and osteogenic (O) *in vitro* differentiation of CD8- and VEGF-expressing ASCs (A, C) and BMSCs (B, D). Expression of the transgene mRNA levels was quantified by qRT-PCR (A, B). VEGF protein in the supernatants (1 mL) was measured by ELISA and normalized for the number of cells and time of incubation (C, D). \*\**p* ≤ 0.01 and \*\*\**p* ≤ 0.001 versus cells cultured in expansion medium (*n* = 3 each). qRT-PCR, quantitative real-time reverse transcriptase PCR; ELISA, enzyme-linked immunosorbent assay.

Previously established clonal populations of skeletal myoblasts transduced with the same ratVEGF-IRES-ratCD8 retrovirus and homogeneously expressing specific VEGF levels<sup>23</sup> were used as reference populations to FACS-sort transduced MSCs expressing similar CD8 levels on the cell surface (Fig. 7A). The unsorted transduced BMSC population expressed on average 142 ± 14 ng/10<sup>6</sup> cells/day of rat VEGF and, after FACS purification, low-, medium-, and high-level sorted populations produced about 12, 79, and 154 ng/10<sup>6</sup> cells/day, respectively. As shown in Fig. 7B, these VEGF amounts were remarkably similar to those produced by the corresponding reference clonal populations (13, 53, and 155 ng/10<sup>6</sup> cells/day, respectively). VEGF secretion by the FACS-purified populations was stable also 5 and 18 days after sorting (data not shown).

**Discussion**

In this study we developed a tool to genetically modify primary human MSCs derived from bone marrow and adipose tissue with high efficiency and rapidly select cells expressing desired levels of VEGF with minimal *in vitro* manipulation, so as to preserve their progenitor properties. This was achieved by combining an optimized transduction

protocol with a high-throughput FACS-based purification technology we recently developed.<sup>29</sup> Neither retroviral vector transduction, nor FACS purification, nor expression of VEGF and the CD8 marker impaired MSC proliferation and *in vitro* differentiation potential toward the adipogenic and osteogenic lineages. Transgene expression was sustained during *in vitro* differentiation. Interestingly, we recently found that similarly transduced and FACS-purified BMSCs, expressing only the truncated CD8 marker, also displayed no impairment of their chondrogenic potential both *in vitro* and *in vivo* (Marsano, A., Martin, I., and Banfi, A., unpublished observations).

The lack of detrimental effects on BMSC properties by VEGF overexpression was not due to a lack of activity of rat VEGF on human VEGF receptors. In fact, rat VEGF<sub>164</sub> shares 90% amino acid sequence identity with human VEGF<sub>165</sub> (<http://blast.ncbi.nlm.nih.gov/>) and is effective in stimulating the proliferation of human endothelial cells,<sup>30</sup> with a similar potency as the corresponding human recombinant factor (ED<sub>50</sub> rVEGF<sub>164</sub> = 0.75–3.75 ng/mL and ED<sub>50</sub> hVEGF<sub>165</sub> = 1–6 ng/mL), according to manufacturer data (R&D Systems).

Genetic modification with integrating vectors, such as retroviruses, ensures consistent long-term expression of

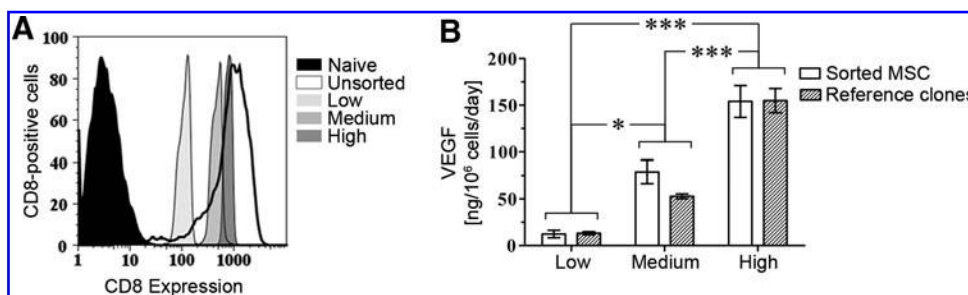


**FIG. 7.** FACS purification of transduced BMSCs expressing specific VEGF levels. Clonal populations of mouse skeletal myoblasts transduced with the same retroviral vector expressing rat VEGF and rat CD8—which produced specific low, medium, and high VEGF levels—were used as reference populations to FACS-

purify VEGF-producing BMSCs that expressed similar levels of CD8 on the cell surface (A). Quantification of rat VEGF<sub>164</sub> by ELISA (B) shows that FACS sorting was successful in rapidly purifying BMSC populations homogeneously producing the same VEGF amounts as the corresponding reference populations. \**p* ≤ 0.05 and \*\*\**p* ≤ 0.001.

factors despite cell expansion.<sup>14</sup> However, current methods for MSC transduction require that standardized proliferating cultures are established by replating MSCs at specific densities after the first confluence is reached,<sup>31–33</sup> so that until now a primary genetically modified population could not be generated before the second passage. In addition, a high transduction efficiency is desirable, so as to minimize the need for selection of the expressing cells and for further expansion to reach the required quantity. Therefore, by rigorously determining the exact time at which freshly isolated MSCs reach the highest proliferative activity after first plating, we were able to target retroviral vector transduction at the most efficient window and achieve a transduction efficiency of up to 95% before first confluence was reached. It should be noted that initial experiments to determine the optimal protocol led to efficiencies of only approximately 70% because they were performed with frozen aliquots of pooled viral vector supernatants in order to ensure standardized conditions. However, fresh supernatants, which have higher titers, allowed the routine achievement of >90% efficiency with the same protocol.

A crucial aspect of the technique we developed is the possibility to rapidly and prospectively purify subpopulations of transduced cells expressing specific desired levels of the transgene. In fact, selection of transduced cells by drug resistance<sup>34</sup> cannot distinguish cells expressing different transgene levels. On the other hand, although single-cell cloning can generate populations expressing precisely controlled levels, it is not a clinically applicable approach due to (1) the excessive degree of *in vitro* expansion required, which is incompatible with the maintenance of differentiation potential of human MSCs; and (2) the excessive costs and complexity associated with generating and screening libraries of clones. Coexpression of a FACS-detectable marker, for example, green fluorescent protein, without the use of reference populations also does not allow the predictive identification of the levels of expression in each cell.<sup>35</sup> In fact, although FACS is intrinsically quantitative, the measured fluorescence intensity values cannot be directly translated into absolute amounts of transgene production. Here we overcame this limitation by taking advantage of a technique we recently developed to predict the absolute amount of expression by individual transduced skeletal myoblasts in a population by FACS, based on the combined use of a syngenic nonfunctional cell surface marker (truncated CD8a) with that of immortal clonal populations as a reference.<sup>29</sup> It can be noted that the CD8 intensity of the high-expressing purified population shown in Figure 7A corresponded to the middle peak of the parent unsorted population and, in fact, the two populations also expressed a similar amount of rat VEGF (142 and 154 ng/10<sup>6</sup> cells/day, respectively), confirming the predictive validity of the platform.

The possibility to control the expressed dose of a transgene has important therapeutic implications. In fact, in a heterogeneous population, high levels can be toxic and low levels inefficient, leading to a waste of therapeutic potential.<sup>10</sup> For example, VEGF overexpression is an attractive strategy to induce therapeutic angiogenesis in ischemic conditions,<sup>36</sup> as well as to increase and accelerate vascularization of clinical-size tissue-engineered grafts.<sup>37</sup> However, VEGF can induce either normal and therapeutic angiogenesis, or aberrant angioma-like vascular growth depending on

its concentration in the microenvironment around each producing cell *in vivo*, and not on its total dose,<sup>11,38</sup> as it remains bound to the extracellular matrix after secretion. Here we showed that MSC subpopulations homogeneously producing specific desired VEGF doses can be rapidly and prospectively purified from the initial transduced population already at the first passage, with no loss of their proliferation and differentiation potential, by combining the optimized transduction protocol and high-throughput FACS-based purification technology we developed. Furthermore, it should prove useful also to study the dose-dependent effects of genes of therapeutic interest on early-passage primary MSCs. In fact, the results obtained studying heterogeneous transduced populations usually reflect the effects of the highest levels of expression, which may obscure those of the lower and more physiological levels.

Interestingly, *in vitro* osteogenic differentiation caused an increased expression of the vector-encoded VEGF in adipose-derived, but not in bone marrow-derived MSCs, which was confirmed in three independent donors (Fig. 6C, D). Cell differentiation involves extensive alterations in gene expression that depend on chromatin remodeling<sup>28</sup> and this influences the transcriptional activity of the retroviral vectors integrated in those genomic areas. Therefore, this different effect on vector activity in ASCs and BMSCs suggests that osteogenic differentiation of MSCs of different origin might involve the activation and repression of different genomic areas. Further transcriptome analyses will be required to investigate this intriguing possibility.

In conclusion, the platform described here is expected to increase the feasibility of therapeutic approaches based on genetically modified MSCs, by ensuring both high efficiency and minimal *in vitro* manipulation.

### Acknowledgments

This work was supported by an Intramural Research Grant of the Department of Surgery (Basel University Hospital), by the European Union FP7 grants MAGISTER (CP-IP 214685) and ANGIOSCAFF (CP-IP 214402), by the Swiss National Science Foundation grant 127426, and by the National Institutes of Health grant R21-HL089913-02 to Andrea Banfi.

### Disclosure Statement

No competing financial interests exist.

### References

1. Satija, N.K., Singh, V.K., Verma, Y.K., Gupta, P., Sharma, S., Afrin, F., *et al.* Mesenchymal stem cell-based therapy: a new paradigm in regenerative medicine. *J Cell Mol Med* **13**, 4385, 2009.
2. Kumar, S., Chanda, D., and Ponnazhagan, S. Therapeutic potential of genetically modified mesenchymal stem cells. *Gene Ther* **15**, 711, 2008.
3. Crisan, M., Yap, S., Casteilla, L., Chen, C.W., Corselli, M., Park, T.S., *et al.* A perivascular origin for mesenchymal stem cells in multiple human organs. *Cell Stem Cell* **3**, 301, 2008.
4. Helder, M.N., Knippenberg, M., Klein-Nulend, J., and Wuisman, P. Stem cells from adipose tissue allow challenging new concepts for regenerative medicine. *Tissue Eng* **13**, 1799, 2007.



5. Salem, H.K., and Thiernemann, C. Mesenchymal Stromal Cells: current understanding and clinical status. *Stem Cells* **28**, 585, 2010.
6. Kneser, U., Stangenberg, L., Ohnolz, J., Buettner, O., Stern-Straeter, J., Mobest, A., *et al.* Evaluation of processed bovine cancellous bone matrix seeded with syngenic osteoblasts in a critical size calvarial defect rat model. *J Cell Mol Med* **10**, 695, 2006.
7. Scheufler, O., Schaefer, D.J., Jaquiere, C., Braccini, A., Wendt, D.J., Gasser, J.A., *et al.* Spatial and temporal patterns of bone formation in ectopically pre-fabricated, autologous cell-based engineered bone flaps in rabbits. *J Cell Mol Med* **12**, 1238, 2008.
8. Scherberich, A., Muller, A.M., Schafer, D.J., Banfi, A., and Martin, I. Adipose tissue-derived progenitors for engineering osteogenic and vasculogenic grafts. *J Cell Physiol* **225**, 348, 2010.
9. Carmeliet, P. Angiogenesis in health and disease. *Nature Med* **9**, 653, 2003.
10. Banfi, A., von Degenfeld, G., Blau, H.M. Critical role of microenvironmental factors in angiogenesis. *Curr Atheroscler Rep* **7**, 227, 2005.
11. Ozawa, C.R., Banfi, A., Glazer, N.L., Thurston, G., Springer, M.L., Kraft, P.E., *et al.* Microenvironmental VEGF concentration, not total dose, determines a threshold between normal and aberrant angiogenesis. *J Clin Invest* **113**, 516, 2004.
12. Dor, Y., Djonov, V., Abramovitch, R., Itin, A., Fishman, G.I., Carmeliet, P., *et al.* Conditional switching of VEGF provides new insights into adult neovascularization and pro-angiogenic therapy. *EMBO J* **21**, 1939, 2002.
13. Sheridan, C. Gene therapy finds its niche. *Nature Biotechnol* **29**, 121, 2011.
14. Zhang, X.J., Godbey, W.T. Viral vectors for gene delivery in tissue engineering. *Adv Drug Deliv Rev* **58**, 515, 2006.
15. Banfi, A., Muraglia, A., Dozin, B., Mastrogiacomo, M., Cancedda, R., and Quarto, R. Proliferation kinetics and differentiation potential of *ex vivo* expanded human bone marrow stromal cells: implications for their use in cell therapy. *Exp Hematol* **28**, 707, 2000.
16. DiGirolamo, C.M., Stokes, D., Colter, D., Phinney, D.G., Class, R., and Prockop, D.J. Propagation and senescence of human marrow stromal cells in culture: a simple colony-forming assay identifies samples with the greatest potential to propagate and differentiate. *Br J Haematol* **107**, 275, 1999.
17. Scherberich, A., Galli, R., Jaquiere, C., Farhadi, J., and Martin, I. Three-dimensional perfusion culture of human adipose tissue-derived endothelial and osteoblastic progenitors generates osteogenic constructs with intrinsic vascularization capacity. *Stem Cells* **25**, 1823, 2007.
18. Horn, P., Bork, S., Diehlmann, A., Walenda, T., Eckstein, V., Ho, A.D., *et al.* Isolation of human mesenchymal stromal cells is more efficient by red blood cell lysis. *Cytotherapy* **10**, 676, 2008.
19. Mueller, A.M., Davenport, M., Verrier, S., Droeser, R., Alini, M., Bocelli-Tyndall, C., *et al.* Platelet lysate as a serum substitute for 2D static and 3D perfusion culture of stromal vascular fraction cells from human adipose tissue. *Tissue Eng Part A* **15**, 869, 2009.
20. Banfi, A., Springer, M.L., Blau, H.M. Myoblast-mediated gene transfer for therapeutic angiogenesis. *Gene Ther Methods* **346**, 145, 2002.
21. Cifone, M.G., Migliorati, G., Parroni, R., Marchetti, C., Millimaggi, D., Santoni, A., *et al.* Dexamethasone-induced thymocyte apoptosis: apoptotic signal involves the sequential activation of phosphoinositide-specific phospholipase C, acidic sphingomyelinase, and caspases. *Blood* **93**, 2282, 1999.
22. Watson, J.V., Chambers, S.H., and Smith, P.J. A pragmatic approach to the analysis of dna histograms with a definable g1 peak. *Cytometry* **8**, 1, 1987.
23. Wolff, T., Mujagic, E., Gianni-Barrera, R., Fueglistaler, P., Helmrich, U., Misteli, H., *et al.* FACS-purified myoblasts producing controlled VEGF levels induce safe and stable angiogenesis in chronic hind limb ischemia. *J Cell Mol Med* 2011 [Epub ahead of print]; DOI: 10.1111/j.1582-4934.2011.01308.x.
24. Springer, M.L., and Blau, H.M. High-efficiency retroviral infection of primary myoblasts. *Somat Cell Mol Genet* **23**, 203, 1997.
25. Frank, O., Heim, M., Jakob, M., Barbero, A., Schafer, D., Bendik, I., *et al.* Real-time quantitative RT-PCR analysis of human bone marrow stromal cells during osteogenic differentiation *in vitro*. *J Cell Biochem* **85**, 737, 2002.
26. Martin, I., Jakob, M., Schafer, D., Dick, W., Spagnoli, G., and Heberer, M. Quantitative analysis of gene expression in human articular cartilage from normal and osteoarthritic joints. *Osteoarthritis Cartilage* **9**, 112, 2001.
27. Mizuguchi, H., Xu, Z.L., Ishii-Watabe, A., Uchida, E., and Hayakawa, T. IRES-dependent second gene expression is significantly lower than cap-dependent first gene expression in a bicistronic vector. *Mol Ther* **1**, 376, 2000.
28. de la Serna, I.L., Ohkawa, Y., and Imbalzano, A.N. Chromatin remodelling in mammalian differentiation: lessons from ATP-dependent remodellers. *Nature Rev Genet* **7**, 461, 2006.
29. Misteli, H., Wolff, T., Fueglistaler, P., Gianni-Barrera, R., Gürke, L., Heberer, M., *et al.* High-throughput flow cytometry purification of transduced progenitors expressing defined levels of vascular endothelial growth factor induces controlled angiogenesis *in vivo*. *Stem Cells* **28**, 611, 2010.
30. Conn, G., Soderman, D.D., Schaeffer, M.T., Wile, M., Hatcher, V.B., and Thomas, K.A. Purification of a glycoprotein vascular endothelial-cell mitogen from a rat glioma-derived cell-line. *Proc Natl Acad Sci U S A* **87**, 1323, 1990.
31. Marx, J.C., Allay, J.A., Persons, D.A., Nooner, S.A., Hargrove, P.W., Kelly, P.F., *et al.* High-efficiency transduction and long-term gene expression with a murine stem cell retroviral vector encoding the green fluorescent protein in human marrow stromal cells. *Hum Gene Ther* **10**, 1163, 1999.
32. Li, H.X., Zuo, S., He, Z.S., Yang, Y.T., Pasha, Z., Wang, Y.G., *et al.* Paracrine factors released by GATA-4 over-expressed mesenchymal stem cells increase angiogenesis and cell survival. *Am J Physiol Heart Circ Physiol* **299**, H1772, 2010.
33. Noiseux, N., Gnechi, M., Lopez-Illasaca, M., Zhang, L.N., Solomon, S.D., Deb, A., *et al.* Mesenchymal stem cells over-expressing akt dramatically repair infarcted myocardium and improve cardiac function despite infrequent cellular fusion or differentiation. *Mol Ther* **14**, 840, 2006.
34. Wolbank, S., Stadler, G., Peterbauer, A., Gillich, A., Karbiener, M., Streubel, B., *et al.* Telomerase immortalized human amnion- and adipose-derived mesenchymal stem cells: maintenance of differentiation and immunomodulatory characteristics. *Tissue Eng Part A* **15**, 1843, 2009.
35. Liu, X.D., Constantinescu, S.N., Sun, Y., Bogan, J.S., Hirsch, D., Weinberg, R.A., *et al.* Generation of mammalian cells

- stably expressing multiple genes at predetermined levels. *Anal Biochem* **280**, 20, 2000.
36. Yla-Herttuala, S., Rissanen, T.T., Vajanto, I., and Hartikainen, J. Vascular endothelial growth factors - Biology and current status of clinical applications in cardiovascular medicine. *J Am Coll Cardiol* **49**, 1015, 2007.
  37. Rouwkema, J., Rivron, N.C., and van Blitterswijk, C.A. Vascularization in tissue engineering. *Trends Biotechnol* **26**, 434, 2008.
  38. von Degenfeld, G., Banfi, A., Springer, M.L., Wagner, R.A., Jacobi, J., Ozawa, C.R., *et al.* Microenvironmental VEGF distribution is critical for stable and functional vessel growth in ischemia. *Faseb J* **20**, 2657, 2006.

Address correspondence to:

*Andrea Banfi, M.D.  
Cell and Gene Therapy  
Basel University Hospital  
ICFS 407, Hebelstrasse 20  
CH-4031 Basel  
Switzerland*

*E-mail: abanfi@uhbs.ch*

*Received: July 21, 2011*

*Accepted: November 8, 2011*

*Online Publication Date: December 19, 2011*

**This article has been cited by:**

1. Uta Helmrich, Nunzia Di Maggio, Sinan Güven, Elena Groppa, Ludovic Melly, Rene D. Largo, Michael Heberer, Ivan Martin, Arnaud Scherberich, Andrea Banfi. 2013. Osteogenic graft vascularization and bone resorption by VEGF-expressing human mesenchymal progenitors. *Biomaterials* **34**:21, 5025-5035. [[CrossRef](#)]
2. Anna Marsano, Robert Maidhof, Jianwen Luo, Kana Fujikara, Elisa E. Konofagou, Andrea Banfi, Gordana Vunjak-Novakovic. 2013. The effect of controlled expression of VEGF by transduced myoblasts in a cardiac patch on vascularization in a mouse model of myocardial infarction. *Biomaterials* **34**:2, 393-401. [[CrossRef](#)]
3. Ludovic F. Melly, Anna Marsano, Aurelien Frobert, Stefano Boccoardo, Uta Helmrich, Michael Heberer, Friedrich S. Eckstein, Thierry P. Carrel, Marie-Noëlle Giraud, Hendrik T. Tevaearai, Andrea Banfi. 2012. Controlled Angiogenesis in the Heart by Cell-Based Expression of Specific Vascular Endothelial Growth Factor Levels. *Human Gene Therapy Methods* **23**:5, 346-356. [[Abstract](#)] [[Full Text HTML](#)] [[Full Text PDF](#)] [[Full Text PDF with Links](#)]